PCCP

Accepted Manuscript

This is an *Accepted Manuscript*, which has been through the Royal Society of Chemistry peer review process and has been accepted for publication.

Accepted Manuscripts are published online shortly after acceptance, before technical editing, formatting and proof reading. Using this free service, authors can make their results available to the community, in citable form, before we publish the edited article. We will replace this *Accepted Manuscript* with the edited and formatted *Advance Article* as soon as it is available.

You can find more information about *Accepted Manuscripts* in the Information for Authors.

Please note that technical editing may introduce minor changes to the text and/or graphics, which may alter content. The journal's standard Terms & Conditions and the Ethical guidelines still apply. In no event shall the Royal Society of Chemistry be held responsible for any errors or omissions in this *Accepted Manuscript* or any consequences arising from the use of any information it contains.

ROYAL SOCIETY OF CHEMISTRY

www.rsc.org/pccp

Ultra-fast and Slow Charge Recombination Dynamics of Diketopyrrolopyrrole-NiO Dye Sensitized Solar Cells

Lei Zhang[a], Ludovic Favereau[b], Yoann Farré,[b] Edgar Mijangos[a], Yann Pellegrin,[b] Errol Blart, [b] Fabrice Odobel[b]* and Leif Hammarström[a]*

[a] *Department of Chemistry, Ångström Laboratory, Uppsala University, Box 523, Uppsala SE75120, Sweden* E-mail: Leif.Hammarstrom@kemi.uu.se

[b] *Université LUNAM, Université de Nantes, CNRS, Chimie et Interdisciplinarité: Synthèse, Analyse, Modélisation (CEISAM), UMR 6230,2 rue de la Houssinière, 44322Nantes cedex 3, France.* E-mail: Fabrice.Odobel@univ-nantes.fr

Abstract: Photophysical study of two diketopyrrolopyrrole (DPP) based sensitizers functionalized with a 4-thiophene carboxylic acid as anchoring group and a bromo (DPPBr) or vinyldicyano (DPPCN2) and a dyad consisting of a DPP unit linked to a naphthalene diimide (DPP-NDI) were investigated both in solution and grafted on mesoporous NiO films. Femtosecond transient absorption measurements indicate that ultrafast hole injection occurred predominantly on a time scale of ~200 fs, while the subsequent charge recombination occurred on a surprisingly wide range of time scales, from tens of ps to tens of μs; this kinetic heterogeneity is much greater than what is typically observed form dye-sensitized TiO_2 or ZnO. Also in contrast to what is typically observed for dye-sensitized TiO_2, there was no significant excitation power dependence of the recombination kinetics, which can be explained by the comparatively higher hole density near the valence band of NiO already before excitation. The additional acceptor group in DPP-NDI provided rapid electron shift and stabilized charge separation out to the μs time scale. This allowed for efficient (~95%) NDI regeneration by the $Co^{III}(dtb)_3$ electrolyte (dtb = 4,4'-di-*tert*butyl-2,2-bipyridine), according to transient absorption measurements. Regeneration of DPPBr and DPPCN2 by $Co^{III}(dtb)_3$ was instead inefficient, as most recombination for these dyes occurred on the sub-ns time scale. The transient spectroscopy data thus corroborated the trend of published photovoltaic properties of dye-sensitized solar cells (DSSCs) based on these dyes on mesoporous NiO, and shows the potential of a design strategy with a secondary acceptor to the dye. The study identifies rapid initial recombination between dye and NiO as the main obstacle to obtaining high efficiencies in NiO-based DSSCs; these recombination components may be overlooked when studies are conducted using methods with ns-resolution or slower.

Physical Chemistry Chemical Physics Accepted Manuscript

Keywords: Photocathode, p-type DSSCs, Nickel oxide, Electron transfer, Tandem cells, Charge separation

Introduction

The design of photosensitizers for p-type semiconductor (p-SC) based dye sensitized solar cells (DSSCs) has drawn attention,[1-14] due to the possible applications in photocatalysis[15-18] and because it is indispensable for the development of the tandem dye sensitized solar cells.[19-24] The photosensitizer is one of the crucial components, which controls the overall performance of the solar cell. Light absorption entails the excited state formation which subsequently injects a hole into the nanoporous NiO film (or other p-SC). A redox mediator such as triiodide or a cobalt[25,26] or iron[27] complex regenerates the dye and delivers electrons to the counter electrode in order to complete the photovoltaic circuit. However, the rapid charge recombination between the injected holes and the reduced sensitizer is much faster in p-DSSCs than conventional DSSCs based on n-SC, such as TiO_2, and occurs in most cases on a less than 1 ns time scale.[13,14] Therefore, in order to achieve highly efficient systems, the charge recombination dynamic processes are the most critical factors to improve, in particular the competition between dye regeneration and recombination of the reduced dye with the hole in NiO. An important strategy to overcome the quite usual fast charge recombination is the development of dye-acceptor dyads to rapidly localize the ejected electron far away from the NiO surface.[22,28,29] Recently, we found that simple diketopyrrolopyrrole based dyes (DPPBr and DPPCN2) and a "D-A" dyad (DPP-NDI are promising sensitizers for p-DSSCs and they can be used with both iodide and cobalt electrolytes (Chart 1).[30] The photovoltaic performances show that the photocurrent increased with the replacement of the bromine group by better acceptor groups: a thiophene-dicyanovinylene or a secondary electron acceptor (NDI), in the presence of an iodide/triiodide electrolyte. When a $Co^{II/III}(dtb)_3(PF_6)_{2/3}$ electrolyte (see structure in Figure S1) was used with the DPP-NDI dyad, both photovoltage

Physical Chemistry Chemical Physics Accepted Manuscript

and photocurrent were greatly improved, and the V_{OC} was twice higher (365 mV vs. 155 mV). Prompted by these interesting photovoltaic performances, we have decided to investigate the detailed mechanism of the charge transfer of these three dyes. Herein, we report a photophysical study of these diketopyrrolopyrrole based sensitizers with time-resolved techniques both in solution and chemisorbed on NiO films. Understanding of all the excited singlet states and triplet states were processed to help us give a clear picture of the charge transfer mechanisms involving the photo-excited dyes adsorbed on the NiO mesoporous films. Femtosecond and nanosecond transient absorption spectroscopy respectively shield some light on the ultra-fast (ps time scale) and slow (ns-μs time scale) charge transfer processes. The obtained results demonstrated that the reduced DPP-NDI$^{\bullet-}$ is regenerated by more than 80% efficiency by the Co^{III} complex, while the other two dyes (DPPBr and DPPCN2) are regenerated to a much smaller extent. This explains the improvement of photovoltaic performance by appending the NDI acceptor to DPP and using the $Co^{II/III}$ electrolyte.[30]

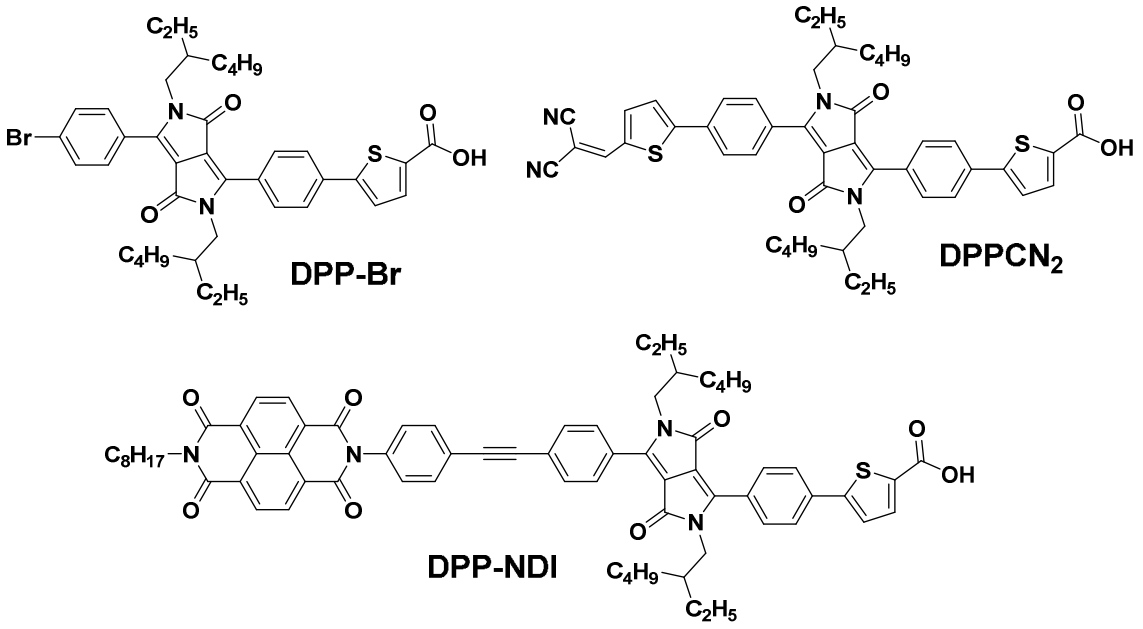

Chart 1. Structures of the diketopyrrolopyrrole based sensitizers investigated in this work.

Physical Chemistry Chemical Physics Accepted Manuscript

Experimental Section

General

The preparation of the dyes DPPBr, $DPPCN_2$ and DPP-NDI were reported in a previous study.[30] Solvents employed for this study (dichloromethane (Aldrich, UV spectroscopy grade), ethanol (Aldrich, 99.5% spectroscopy grade), propylene carbonate (Aldrich, 99% ACS reagent grade) were used without further purification unless otherwise noted. The preparation of $Co^{II/III}(dtb)_3$ (dtb = 4,4'-di*tert*butyl-2,2'-bipyridine) used as redox mediator was published elsewhere.[30]

For spectroscopic measurements on solution samples, a quartz cuvette with 1 cm path length was used (1 mm for the fs experiments), unless otherwise noted. The sensitized NiO samples were prepared as described below.

Spectroelectrochemical characterization

Spectroelectrochemistry was performed in a three-electrode electrochemical cell with a platinum mesh working electrode, glassy carbon counter electrode and $Ag/AgNO_3$ (10 mM/MeCN) as reference electrode. The electrochemical cell was set up in a quartz cuvette with an optical pathway of 1 mm. The sample was dissolved in a 0.1 M t-Bu_4NPF_6 / DCM electrolyte solution. The counter electrode was kept separate from the main solution by a salt bridge with glass frit tip. The potential was applied with an Autolab PGSTAT302 potentiostat/galvanostat, while the spectra were acquired with an Agilent 8453 UV-Vis spectrophotometer. Experiments were carried out in a glovebox (MBraun) maintained at < 0.1 ppm O_2.

Physical Chemistry Chemical Physics Accepted Manuscript

NiO film preparation

Preparation and assembly of the sandwich solar cells followed methods previously described.[31] 3 g $NiCl_2$ (Sigma-Aldrich) anhydride and 1 g F108 polymer (Sigma-Aldrich) were dissolved in a mixture of 9 g of deionized water and 18 g of 99.5% of ethanol. The resulting green viscous solution was sonicated overnight. The mixture was centrifuged for 15 min to sediment out undissolved $NiCl_2$ and amorphous NiO. After centrifugation, the supernatant was collected as three separate batches for use as doctor-blading paste. Mesoporous NiO electrodes were prepared by spreading the doctor-blading paste onto conducting F-doped SnO_2 (FTO) glass masked with adhesive tape and sintered in a furnace at 450 °C for 30 minutes.

Sensitization of NiO film for spectroscopic characterization

The sensitizing solutions were ~0.05 mM solutions (3:1 dichloromethane: ethanol) of the desired sensitizer. NiO films supported on microscope slides were heated to 50 ℃ overnight and placed into sensitized solutions while warm. Films were allowed to soak in the sensitizing solution for 16 hours in a dark cupboard. Immediately prior to measurements the films were removed from the sensitizing solution and rinsed with dichloromethane. After drying the film in a stream of nitrogen a drop of propylene carbonate (PC) solvent was placed onto the film and a clean piece of glass slide placed onto to create a sandwich cell configuration. Capillary forces enable the covering glass to adhere to the glass substrate possessing the sensitized film. Typical optical densities of the sensitizer on the NiO were 0.3-0.6.

Steady state absorption and fluorescence

Steady state absorbance spectra were collected with a Cary 50 UV-Visible spectrophotometer.

Physical Chemistry Chemical Physics Accepted Manuscript

Emission spectra were collected with a FluoroLog emission spectrometer. Solution phase samples were measured in quartz cuvettes with the desired solvent. Optical densities of samples for emission spectroscopy were on the order of 0.1, while those for solution phase and NiO films ultrafast measurements were between 0.3 and 0.6.

Time-correlated single photon counting (TCSPC)

The detailed description of the experimental setup has been given recently.[32] Briefly, the sample was excited with a picosecond diode laser (Edinburgh Instruments, EPL470) at 470 nm (77.1 ps pulses) The laser pulse energy was ca. 15 pJ and was attenuated (often more than 1 order of magnitude) to the desired count rate of 1% or less of the excitation frequency.

Decay curves obtained by single photon counting were analyzed by iterative reconvolution using an exponential decay model with 1 or 2 components in the SpectraSolve program. The instrument response function (IRF: 60 ps) was free to move relative to the decay during analysis.

Nanosecond transient absorption spectrometer

The sample was excited by a Q-switched YAG-laser/MOPO combination (Spectra Physics) that delivered ca. 10 ns pulses at 10 Hz repetition frequency. The pulses were attenuated to 1-10 mJ/pulse over ca. 0.3 cm^2. The spectrometer (Edinburgh Instruments) was coupled to a probe light from a pulsed Xe-lamp (long pass filtered at 380 nm) at a 90 degree angle from the laser excitation, while the sample was placed at 45 degrees with respect to both beams for sensitized NiO films or in 1 cm cuvettes for the solution samples. Kinetic traces were recorded using a PMT and a digital oscilloscope. Transient spectra were detected with a CCD (ANDOR).

Physical Chemistry Chemical Physics Accepted Manuscript

Ultrafast femtosecond transient absorption spectrometer

Femtosecond time-resolved measurements were done by means of transient absorption. For a detailed description, see Petersson et al.[33] Briefly, the output from a Coherent Legend Ti:Sapphire amplifier (1 kHz, λ = 800 nm, fwhm 100 fs) was split into a pump and a probe part. Desired pump wavelengths were obtained with a TOPAS, and with neutral density filters the energy of each pulse was kept between 150 and 500 nJ over ca. 3 mm^2. The white light continuum probe was obtained by focusing part of the 800 nm light on a moving CaF_2 plate. Polarization of the pump was set at magic angle, 54.7º, relative to the probe. Instrumental response time depends on pump and probe wavelengths, but is typically about 150 fs. The sample was moved vertically to avoid photodegradation. Several consecutive scans of the optical delay line were measured for each sample. There was no difference in result between the first and last scan, showing that sample degradation was negligible.

Data analysis are done in MATLAB (The MathWorks, Inc.), a robust trust-region reflective Newton nonlinear-least-squares method is used for the fits of time traces. Traces (ΔA vs. t) are fitted to a sum of exponentials convolved with a Gaussian shaped response. Also included in the fits is an artifact signal that is due to cross phase modulation during pump and probe overlap. All spectra are corrected for chirp in the white light probe, time zero is set at maximum pump-probe temporal overlap. The region around pump wavelength is removed due to scatter of pump light (500-550 nm).

Results and Discussion

Absorption and fluorescence measurements

Physical Chemistry Chemical Physics Accepted Manuscript

The spectral features of DPPBr, $DPPCN_2$ and DPP-NDI dyes in solution and on NiO films were first investigated by performing steady-state absorption and fluorescence measurements. Figure 1 shows the UV-vis absorption and fluorescence spectra of DPPs on NiO/FTO films. The steady state absorption and fluorescence spectra of DPPs recorded in dichloromethane (DCM) have been published in previous paper (Figure S2).[30] Time-resolved emission (TCSPC) decays for all three dyes were fitted with double exponential function (Figure S3), which show that the fluorescence lifetimes decreased with increasing electron withdrawing ability of the DPP substituent: from DPPBr (τ = 9.65 ns, 89%) to DPPCN2 with a conjugated acceptor group (τ = 0.78 ns, 88%) and DPP-NDI with a non-conjugated, separate secondary electron acceptor (NDI) (τ = 260 ps, 96%).

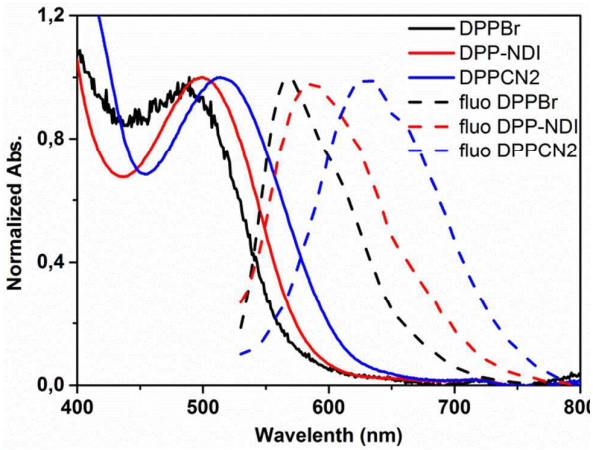

Figure 1. Normalized absorption and emission spectra of DPP based sensitizers recorded on mesoporous NiO films.

Figure 1 shows a broadening of the absorption spectra of DPPs sensitized NiO films in the visible region (400-650 nm) compared to those in solution (Figure S2), which is attributed to the electronic coupling of the dye with the semiconductor surface and probably the formation of aggregates upon immobilization on NiO surface. Broadening of the dye absorption spectra on a metal oxide has previously been observed for many dyes on NiO and TiO_2.[1,34-36] All three photocathodes were found to be photoluminescent. Most dyes inject holes in ~200 fs

Physical Chemistry Chemical Physics Accepted Manuscript

(see below), therefore, the emission is mainly from the fraction of dyes, that for some unknown reasons, slowly inject; similar heterogeneous is typically observed for dye-sensitized TiO_2.[37] Binding on NiO induces a 50 nm red-shift of the emission maximum (peak from 580 nm DCM to 630 nm on NiO). NiO/DPP-NDI shows a similar red shift. This is assignable to the aggregation of molecular dyes on the surface of NiO. In addition, the maximum emission peak of DPPBr shifts from 680 nm in DCM to 665 nm after binding onto the NiO films. The emission band of adsorbed DPPCN2 is thinner than in solution phase in DCM (Figure S2): this is attributed to excited state twisting (see below) that is hindered by the absorption on the NiO surface.

Determination of anion spectra of the DPP dyes

The spectra of the reduced DPP dyes were determined for interpretation of the transient experiments below. The irreversibility of DPP reduction under electrochemical conditions precluded spectroelectrochemical determination of the radical anion absorption spectrum. Instead, we used the nanosecond laser flash-quench method in the presence of an external electron donor, triethylamine (TEA) or $Co^{II}(dtb)_3$. The difference spectra of DPPBr and DPPCN2 recorded with TEA solution added in Ar saturated DCM, Figure S4a, shows a clear difference from those of the dye excited states in DCM (see below). In addition to ground state bleach, there is a positive absorption band at ~430 nm and another broad band at >550 nm. As the signal was very weak, experiments with Co^{II} as electron donor was used to confirm this radical anion spectrum, with similar and higher intensity (Figure S4b).

The first reduction of DPP-NDI is localized on the NDI unit and should be electrochemically reversible.[30] Therefore, the difference absorption spectrum of reduced DPP-NDI in DCM solution was collected by using a spectroelectrochemistry. The DPP-NDI was reduced by applying a bias at -1.0 V versus Ag/AgCl reference and the reduced NDI exhibits a board

Physical Chemistry Chemical Physics Accepted Manuscript

absorption in the visible region with a distinct peak at 475 nm, a weak and broad absorption peak at 610 nm (Figure 2). This spectrum feature is in good agreement with the reported NDI^- absorption in the literature[38] and confirms that the first reduction of DPP-NDI is on the NDI group.

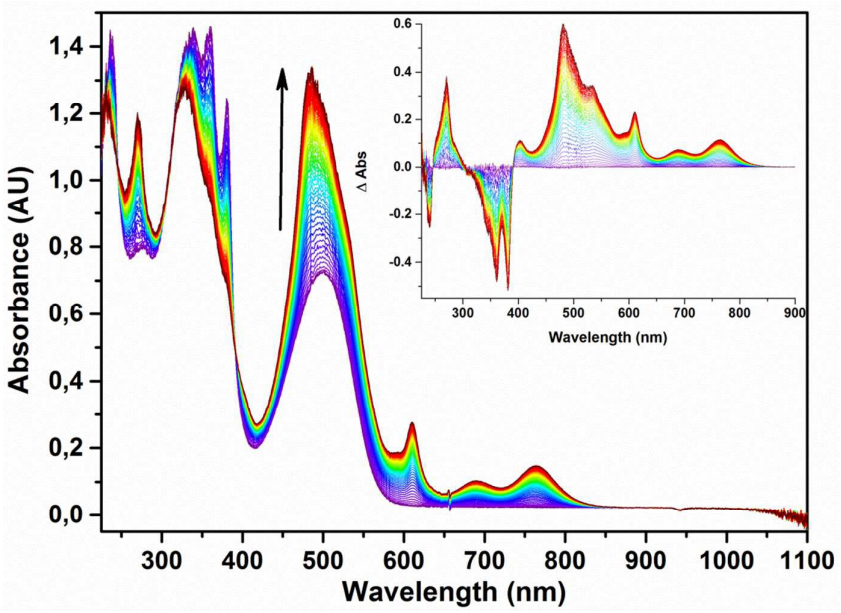

Figure 2. Spectroelectrochemical measurements of DPP-NDI upon reduction at -1.0 V *vs.* Ag/AgCl in dichloromethane (DCM); the arrow indicates the changes observed. Inset: the spectral data plotted as difference spectra.

Transient absorption in solution

The three dyes were then investigated in solution by femtosecond and nanosecond transient absorption spectroscopy to determine spectra for their excited singlet and triplet states for the interpretation of the spectra recorded on NiO surface. Femtosecond transient absorption spectra of DPPBr in DCM, after exciting in the middle of the lowest S_0 - S_1 absorption band, are shown in Figure 3a. The initially formed singlet excited state of DPPBr presents an absorption peak around 400 nm and an absorption band at >650 nm, in addition to ground

Physical Chemistry Chemical Physics Accepted Manuscript

state bleach (GSB) around 475 nm. The stimulated emission shows a strong dynamic Stokes shift with a time constant of ca. 1.5 ps, which is mainly caused by the solvent relaxation, and causes the initial broad and negative signal from 450 - 650 nm to separate into distinct bleach and stimulated emission bands, respectively. Following this dynamics, the emission decays predominantly with a lifetime >1.2 ns, in agreement with the TCSPC results. Kinetic traces at significant wavelengths for DPPBr and DPPCN2 are shown in Figure S5, and for DPP-NDI in Figure 4. The results from a global fit with three time constants are given in Table 1. For DPPBr, the contribution of the intermediate component (97 ps) is small at most wavelengths.

Transient absorption spectra on the nano- and microsecond time scale after excitation with a 10 ns laser flash are shown in Figure 4 for the DPPBr dye with, a time scale when the singlet excited state has already decayed. The transient spectrum is also different from the singlet excited spectrum; most notable is the absence of emission (see endnote[#]), the absorption band that peaks at 560 nm and the absorption band around 380 nm. The transients decay with τ ~10.8 μs in Ar-purged DCM, while it is strongly quenched to 320 ns in air-saturated solvent (Figure 5b). All these features are consistent with a triplet excited state, formed by intersystem crossing from the singlet excited state.

Table 1 Time constants obtained from global analysis of femtosecond transient absorption data for the dyes in DCM solution.

	τ_1 (ps)	τ_2 (ps)	τ_3 (ps)
DPPBr	1.5 ± 0.6	97 ± 3	1200 ± 90
DPPCN2	2.0 ± 0.3	62 ± 12	780 ± 50
DPP-NDI	0.84 ± 0.28	11 ± 4	140 ± 20

Physical Chemistry Chemical Physics Accepted Manuscript

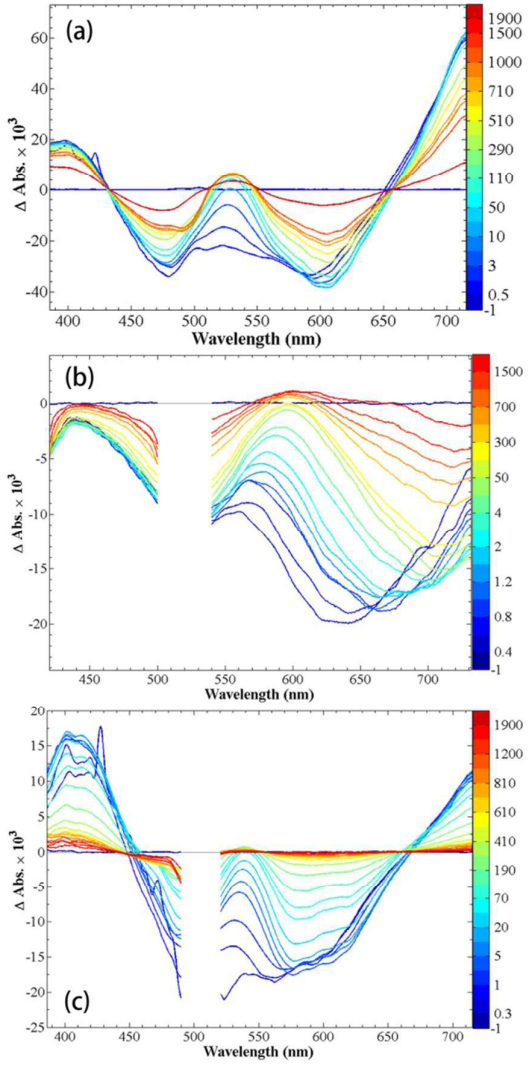

Figure 3. Transient absorption spectra of DPP sensitizers in DCM solution, (a) DPPBr, (b) DPPCN2 and (c) DPP-NDI (time unit: ps). λ_{ex} = 505 nm (520 nm for DPPCN2).

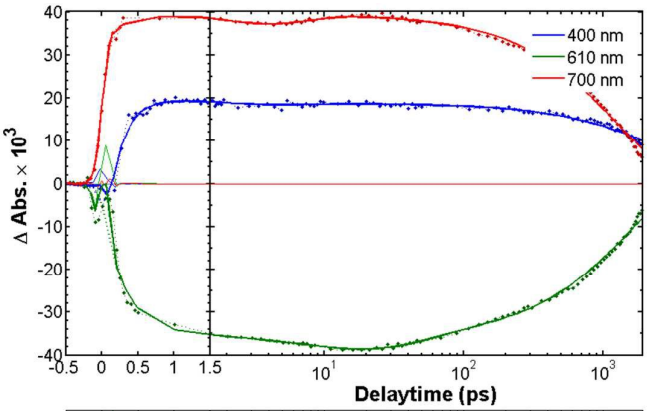

Figure 4. Transient absorption decay traces for DPP-NDI in DCM after excitation at 505 nm.

Physical Chemistry Chemical Physics Accepted Manuscript

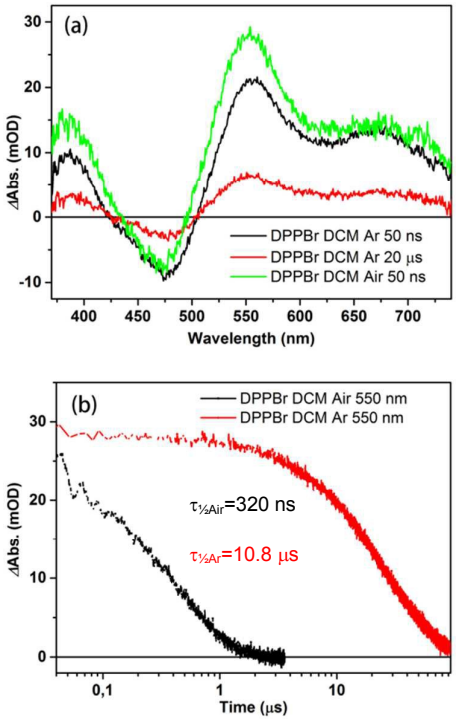

Figure 5. Nanosecond time-resolved transient absorption spectra upon excitation at 532 nm of the DPPBr (a) in DCM with and without argon and (b) the kinetic traces comparison of DPPBr probed at 550 nm.

In the case of DPPCN2 (Figure 3b), the fs-spectra show a strong dynamic Stokes shift of the stimulated emission, with an initial change from 640 nm to 670 nm on a time scale of a few ps. However, the shift continues until most of the transient signal has decayed, out to 2 ns, which also explains the broad fluorescence spectrum in solution (Figure S2). This is much too long for solvent dynamics, and we tentatively ascribe this to the twisting of the dicyanovinyl group in the excited state, similar to other conjugated cyanovinyl dyes.[39] Most of the ground state bleach recovers with a 785 ps time constant, which is in excellent agreement with the TCSPC results (780 ps). The nanosecond transient absorption spectra show absorption beyond 550 nm with a peak at ~685 nm (Figure S6), with lifetimes of 2.9 us (Ar) and 280 ns (air), which was assigned to the triplet excited state of DPPCN2.

Physical Chemistry Chemical Physics Accepted Manuscript

Finally, for DPP-NDI the fs-transient spectra are initially very similar to those for DPP, but the signal decay is faster (Table 1). After *ca.* 1 ns a clear peak at 475 nm is seen within the ground state bleach, which can be attributed to formation of $NDI^{\bullet-}$. Nevertheless, most of the spectrum has the appearance of the excited state and decays predominantly with τ_{CS} = 120 ps. The shorter lifetime compared to DPPBr can be ascribed to intramolecular electron transfer to the NDI unit, forming the $DPP^{\bullet+}$-$NDI^{\bullet-}$ state. However, the subsequent charge recombination is faster, τ_{CR} = 10 ps, which is seen in particular as a rising component at 480 nm (Figure 3c). It is well known for consecutive reactions where the second step is faster than the first, that the signal of the intermediate (counter-intuitively) rises with the time constant of the recombination and decays with that of the charge separation (see any textbook on chemical kinetics). On the ns time scale a spectrum attributable to the DPP-centered triplet is again observed (Figure S6), but with smaller amplitude than for DPPBr because of rapid charge separation and recombination to the ground state. Its lifetime in Ar- and air-saturated solution was similar to that for DPPCN2.

Transient absorption of dye-sensitized NiO films

The dye-sensitized NiO films for transient absorption spectroscopy were coated by propylene carbonate and covered with thin glass slides. The transient absorption spectra (chirp corrected) and selected time traces after ~120 fs excitation around 525 nm with ~500 nJ/pulse are shown in Figures 6-8.

Physical Chemistry Chemical Physics Accepted Manuscript

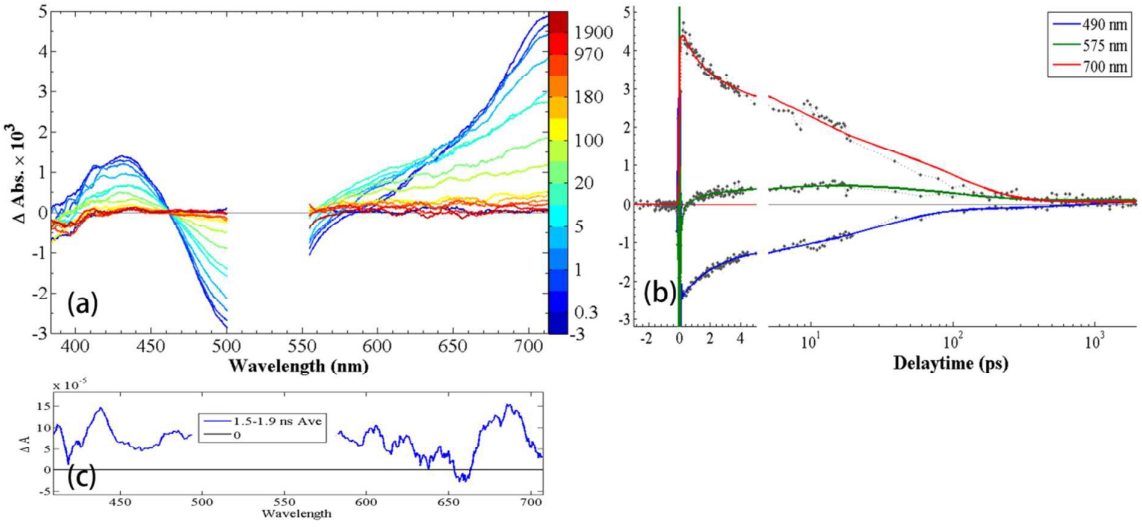

Figure 6. (a) Transient absorption spectra and (b) kinetic traces of NiO/DPPBr excited at 525 nm. (c) the spectra after 1500 - 1900 ps on an expanded scale.

The initial transient absorption spectra of both NiO/DPPBr (Figure 6a) and NiO/DPPCN2 (Figure 7a) show positive absorbance at ~440 nm and >600 nm, ground state bleach around 520 nm and stimulated emission around 600 nm, significant for the singlet excited dye. The signals rapidly decay, in particular the stimulated emission, which leads to a blue shift of the isosbestic point to ~560 nm. This is attributed to the formation of $DPP^{\bullet-}$ by hole injection from $^{1*}DPP$ to NiO with a time constant of 200-400 fs with slower injection components around 1-15 ps, all leading to the formation of the charge separation state NiO^{+}/ $DPP^{\bullet-}$ (Table 2). The resulting spectrum is similar to the reference spectrum for $DPP^{\bullet-}$ obtained with the TEA electron donor in solution (Figure S4). This spectrum decays almost completely within 2 ns, as represented mostly by the slow component in Table 2 (τ = 75 ps and 94 ps, respectively). This is assigned to charge recombination of the $DPP^{\bullet-}$ dye anion with holes in NiO.

Physical Chemistry Chemical Physics Accepted Manuscript

In the case of NiO/DPP-NDI, (Figure 8a) the initial transient absorption spectra are very similar to those for NiO/DPPBr, again showing hole injection from ^{1*}DPP to NiO on ~200 fs time scale, with a slower component represented by a ~2 ps lifetime. However, the slower injection occurs on a time scale overlapping with further electron transfer from $DPP^{\bullet-}$ to the NDI acceptor, represented by the 2 ps and 13 ps components (Table 2). The isosbestic point around 470 nm seen for the other dyes is lost, and the 475 - 500 nm region shows a positive signal already after 1 - 20 ps (Figure 8). As the electron shifts from $DPP^{\bullet-}$ to $NDI^{\bullet-}$, the transient absorption peak at 440 nm changes to 480 nm and the red part absorbance changes to form peak 610 nm, which is in good agreement with the published reduced $NDI^{\bullet-}$ absorption and spectroelectrochemistry result (Figure 2). An important contrast to the fs spectra for the other two dyes on the NiO, NiO/DPP-NDI is that a much larger signal remains after 2 ns time delay. As we do not know the relative extinction coefficients for the $DPP^{\bullet-}$ and $NDI^{\bullet-}$ radicals, we cannot deduce the yield of $NDI^{\bullet-}$ formation. However, the signal around 480 nm rises until *ca.* 20 ps and then remains constant until at least 2 ns (Figure 8b), indicating that there is no recombination of $NDI^{\bullet-}$ and NiO holes on the < 2 ns time scale, and all possible recombination losses would be due to $DPP^{\bullet-}$ and NiO holes before the electron transfers to the NDI unit.

A global fit with a sum of five exponentials (of which one has infinite lifetime) were applied to the data in Figure 6, 7 and 8, see the decay associate spectra (DAS) and recalculated species associate spectra (SAS) in Figure S7, S8 and S9. As we know, the multi-exponential fit to data for this type of system with heterogeneous kinetics is an approximation to illustrate the time scales of a process rather than being precise numbers. The DAS and SAS from global analysis of the data can aid in interpreting the processes of electron transfer and the transient absorbance shape for each species. The τ_1 ~ 200-400 fs DAS and SAS are noisy due to early-time artifacts; nevertheless stimulated emission decay is obvious, supporting our assignment

Physical Chemistry Chemical Physics Accepted Manuscript

to hole injection. The relatively slow, τ_4-component of NiO/DPPBr and NiO/DPPCN2 shows instead clear signatures of $DPP^{\bullet-}$ recombination (*cf.* Figure S4). The intermediate time scale τ_2- and τ_3-component SAS and DAS can be described as a mixture of those for τ_1 and τ_4 in different proportions and are assigned to slow injection (τ = 1-20 ps) in parallel to fast recombination components; injection and recombination are frequently found to overlap in time in NiO/dye systems, reflecting their heterogeneous kinetics. [4,55] For the faster, $\tau_2 \approx$ 1-2 ps, component hole injection dominates, as is also clear from the continued rise of the trace in the region of stimulated emission (575 nm and 610 nm for DPPBr and DPPCN2, respectively, Figures S7-8) until about 20 ps. For NiO/DPP-NDI instead, (Figure S9) the slower components are consistent with the presence of a long-lived $NDI^{\bullet-}$, as discussed above.

Table 2 Time constants obtained from global analysis of dyes on NiO with PC (relative amplitudes at different wavelengths are given in the form of the DAS in Figures S7 – S9)..

	τ_1 (ps)	τ_2 (ps)	τ_3 (ps)	τ_4 (ps)	τ_5 (ps)[a]
DPPBr	0.18 ± 0.03	1.9 ± 0.2	8.6 ± 0.4	75 ± 3	∞
DPPCN2	0.19 ± 0.08	1.2 ± 0.3	6.1 ± 2.1	94 ± 30	∞
DPP-NDI	0.20 ± 0.07	1.9 ± 0.3	13 ± 2	260 ± 28	∞

a) This component is very small for DPPBr and DPPCN2.

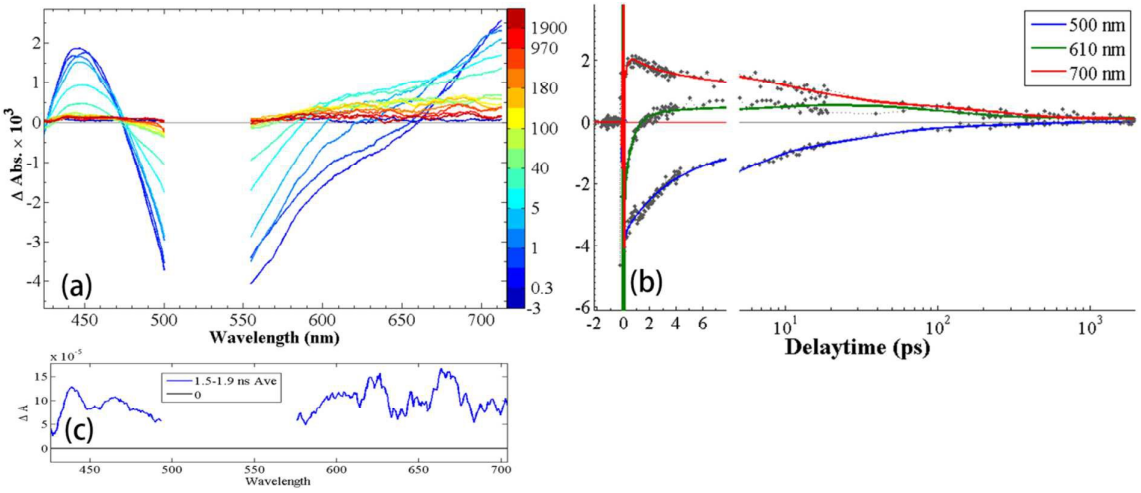

Figure 7. (a) Transient absorption spectra, and (b) kinetic traces of NiO/DPPCN2 excited 525 nm. (c) spectra after 1500 - 1900 ps on an expanded scale.

Physical Chemistry Chemical Physics Accepted Manuscript

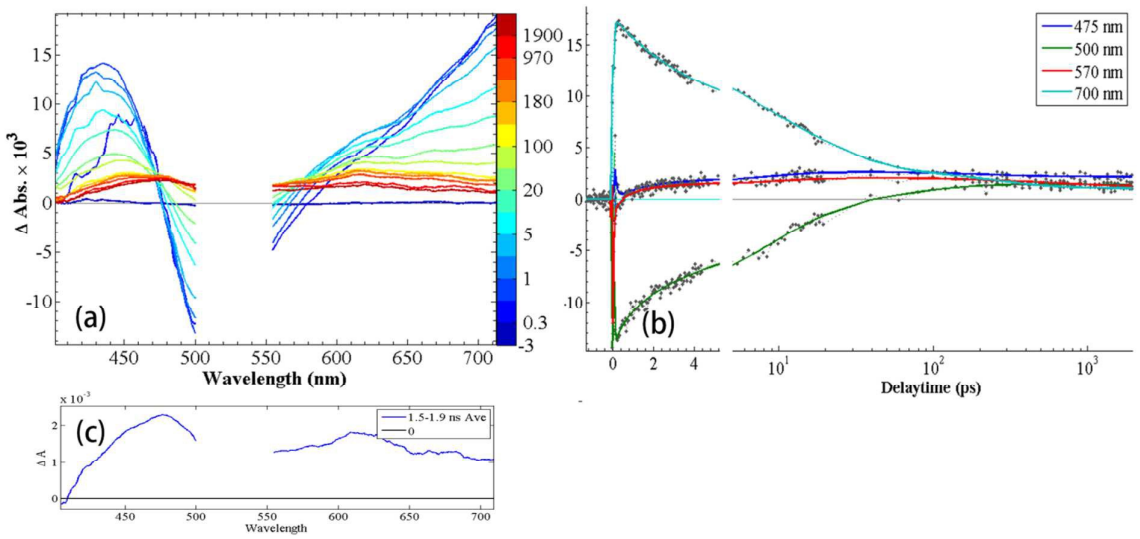

Figure 8. (a) Transient absorption spectra, and (b) kinetic traces of NiO/DPP-NDI excited 525 nm. (c) spectra after 1200 -1900 ps on an expanded scale.

In a summary of the ultrafast transient absorption results, we have shown that all dyes on NiO give ultrafast hole injection (τ = 200-400 fs), also followed by slower, ps components. Ultrafast charge recombination of $DPP^{\bullet-}$ with NiO holes was also found, predominantly on the ~100 ps time scale but with a small fraction (<5%) on the > 1 ns time scale. The secondary charge acceptor in DPP-NDI leads to formation of $DPP\text{-}NDI^{\bullet-}$, which strongly retards the charge recombination process. The long-lived $NDI^{\bullet-}$ signal (> 1 ns) will be discussed in detail in connection to the ns transient results below.

Slow recombination detected by nanosecond transient absorption

The ns transient absorption spectra after 100 ns for all dyes on NiO (in 0.1 M $LiClO_4$, propylene carbonate) are shown in Figure 10 and Figure S13 (laser power: 10 mJ/pulse). The spectral shapes are all in agreement with both the fs transient absorption result and with the reduced state of the dye in solution, see above. The 475 nm and 610 nm absorption peaks for NiO/DPP-NDI represent the radical anion of NDI^{-}, while the peaks around 560 nm, 690 nm

Physical Chemistry Chemical Physics Accepted Manuscript

and 730 nm for the other two samples can be attributed to the absorption of $DPP^{\bullet -}$. Thus, a significant fraction of the reduced dye remains on the 100 ns time scale.

Pump power dependence: The fs results above show that only a small fraction of signal (~1%) remains after 2 ns time delay for NiO/DPPBr and NiO/DPPCN2. Nevertheless, as presented above, a significant signal attributable to $DPP^{\bullet -}$ was observed in the ns measurements (see also Figures 9, S10 and S11). This can be attributed to the higher pump-power density used in the ns-experiments (a few mJ/pulse over ~0.5 cm^2 spot size) than in the fs-experiments (a few hundred nJ/pulse over ~0.001 cm^2 spot size. To investigate if this is a simple linear effect of exciting more of the sample in the ns-experiments, or if non-linear effects were important, experiments were repeated at different pump powers. Figure 9 shows the fs and ns power dependence for NiO/DPPBr. Both sets of experiments gave a linear relationship of ΔAbs. *vs.* laser power, and the traces overlapped well when normalized at the initial signal (Figure S12). This suggests that charge recombination is not affected by the pump power, and that the fraction of slow recombination is essentially independent on laser power; obviously, however, at low power densities the smaller, slow parts of the signal become difficult to distinguish from the noise. Similar results for the pump power dependence were also found for NiO/DPPCN2 and NiO/DPP-NDI (Figure S10). Wood et al. also reported that the charge recombination lifetimes of two organic dyes on NiO did not change significantly with laser pump power, although the dependence of the TA amplitudes was not reported.[8b]

The absence of a power dependence for charge recombination is an important result. First, the linear power dependence also suggests that the results obtained here are relevant under solar irradiation conditions, and is thus useful to analyze photovoltaic data for complete cells. Second, it means that the fraction of slow recombination for NiO/DPPBr and NiO/DPPCN2

Physical Chemistry Chemical Physics Accepted Manuscript

observed is not an artifact, but that recombination occurs over a surprisingly wide range of time scales in the present systems, from a few ps to at least tens of μs. D'Amario *et al.* recently analyzed recombination of a NiO/Ru-dye system on a 10 ns – 1 s time scale with a stretched exponential (KWW) function, resulting in β-values of 0.10-0.15,[40] which is already much smaller than for typical TiO_2/dye systems (0.25-0.4),[41-44] *i.e.* recombination in NiO/Ru-dye occurs over a much wider distribution of time scales. The present data suggests at least an equally broad distribution of recombination time scales, but starting already on the short ps time scale. Third, the independence of recombination on excitation power is very different from what is known for TiO_2/dye systems, where the recombination rate increases drastically with higher excitation powers.[45] D'Amario *et al*[40] suggested that this difference is because NiO already has a high density of holes in the valence band edge region before excitation, while the electron trap density in TiO_2 is comparatively small.

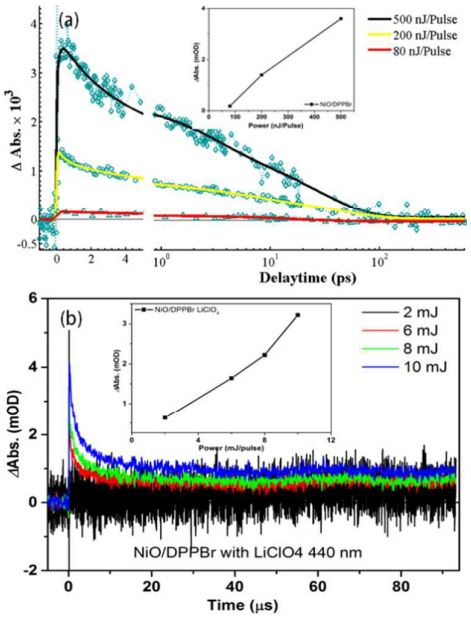

Figure 9. Transient absorption traces for NiO/DPPBr at different laser pump powers: (a) probed at 710 nm after fs-excitation (~ 0.08-0.5 mJ/cm^2); (b) probed at 440 nm after ns-excitation (~ 2-10 mJ/cm^2). The insets show the initial signal as a function of pump intensity.

Physical Chemistry Chemical Physics Accepted Manuscript

Prolonged charge separation in DPP-NDI: The majority of charge recombination in NiO/DPPBr and NiO/DPPCN2 occurs with a lifetime of 65 ps and 150 ps, respectively, as shown by the fs-experiments above. The decay of the signal that remains on the ns – μs time scale (Figures 9, S10) can be fitted by a biexponential function with τ_1 = 1.5-2 μs and τ_2 = 25-30 μs, with roughly equal amplitudes (Table 3). Charge recombination of the $NDI^{\bullet-}$ signal in NiO/DPP-NDI is remarkably slow in comparison: no significant decay is observed up to 2 ns in the fs-experiments, and the ns-experiments show significant decay only from 1 μs to 1 ms (Figure 10). A biexponential fit to the data in Figure 10 resulted in τ_1 = 49 μs (37% amplitude) and τ_2 = 260 μs (63%). The weighted average of logarithmic lifetimes (eq. 1) then gives $\langle\tau\rangle$ = 140 μs. In contrast, for DPPBr and DPPCN2 $\langle\tau\rangle$ is < 500 ps, as the μs components contribute less than 10% to the total decay. Thus, the secondary acceptor unit NDI results in a five orders of magnitude increase in average lifetime. This is in line with previous reports of a PMI-NDI dyad[22,46], but here the resulting lifetime is even another order of magnitude longer. The excess electron on the DPP dye is moved 15-20 Å away from the NiO linker group by electron transfer to the NDI unit (as judged from the center of the LUMO distributions in DPPBr and DPP-NDI[30]). If recombination occurs mainly by through-bond electron transfer, this distance and an attenuation factor $\beta \approx 0.5$ $Å^{-1}$ is sufficient to rationalize the increase in lifetime.[47,48]

Note that we found no evidence for the distinct dual recombination suggested by d'Amario *et al.* for recombination of a Ru(II)-polypridine-naphtalene monoimide dye on NiO.[40] They reported a fast, exponential recombination with $\tau \approx 15$ ns, followed by a much slower recombination represented by a stretched exponential decay. The relative amplitudes of these kinetic phases varied with applied bias. The authors therefore proposed that the rapid recombination occurred in parallel to a hole relaxation mechanism that slowed down recombination. The traces in Figure 9 and S10 for the present DPP dyes, however, show no

Physical Chemistry Chemical Physics Accepted Manuscript

sign of recombination on a ~15 ns time scale. One explanation for the differences compared to ref. 40 could be that the present systems do not show recombination on the right time scale for the proposed relaxation effect to be observed: for DPPBr and DPPCN2 almost all recombination occurred already within 1 ns, while in DPP-NDI almost no recombination occurred before 1 μs.

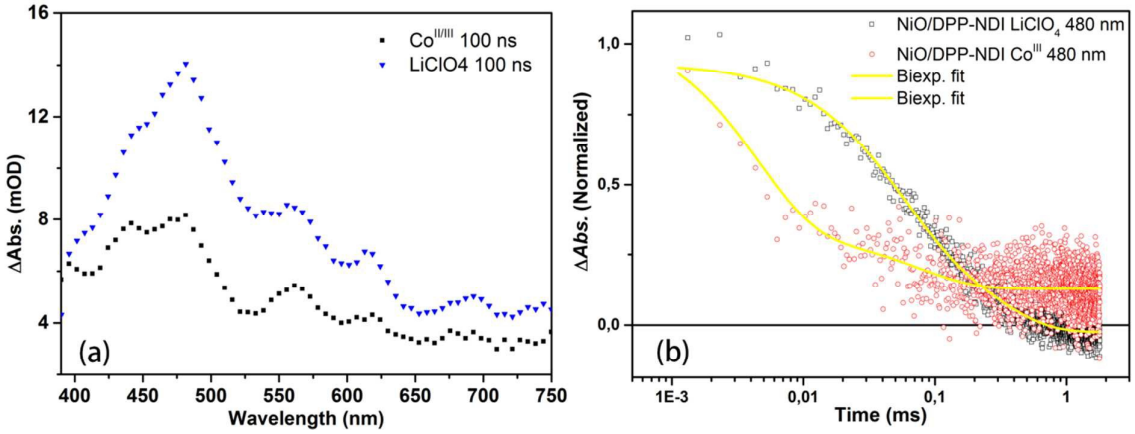

Figure 10. Nanosecond transient absorption spectra (a) and kinetic traces (b) of recombination and regeneration of NiO/DPP-NDI in the presence of $LiClO_4$ and $Co^{II/III}$ after excitation at 532 nm. (traces were monitored at 480 nm with laser power around 10 mJ/pulse).

Regeneration and Interpretation of photovoltaic properties

A $Co^{II/III}(dtb)_3(PF_6)_{2/3}$ (dtb = 4,4'-di*tert*butyl-2,2'-bipyridine) electrolyte was added to investigate the regeneration efficiency for NiO based dye sensitized solar cells. This electrolyte has given comparatively good results in NiO-based DSSCs, provided the dye-NiO charge recombination is slow enough.[22,30] The transient absorption data for NiO/DPP-NDI (Figure 10) shows much faster decay of the $NDI^{\bullet-}$ signal than in plain $LiClO_4$ electrolyte. The effect on the μs decay of $DPP^{\bullet-}$ signal in NiO/DPPBr and NiO/DPPCN2 is in contrast very small (Figure S13).

Physical Chemistry Chemical Physics Accepted Manuscript

To approach a quantitative comparison of the data for the different dyes, and with and without $Co^{II/III}$, we used the weighted average of logarithmic lifetimes from a biexponential fit to the data (eq. 1):[49]

$$log(<\tau>) = \sum A_i \, log(\tau_i) \qquad (1)$$

where A_i is the fractional amplitude for each component. The more common definition of average lifetime, $<\tau> = \sum A_i \, \tau_i$ overemphasizes longer lifetime components and has the related, unsatisfactory problem that $<\tau> \neq (<k>)^{-1}$. These two problems are solved by the definition in eq. 1, which gives equal weight to each decadic time scale just like plots of data on a logarithmic time scales do. We emphasize again, however, as we did in connection to the fs-data above, that a sum of exponents fit for these heterogeneous systems is an approximation to describe the time scales of a process rather than giving precise numbers. While there is most probably an underlying exponentiality to the recombination process, each lifetime derived will not describe a discrete exponential process.

Fits using the KWW-function (stretched exponential, eq. 2)[45,50-52] that is commonly used in DSSC research gave worse fits to our data.

$$Abs(t) = Abs(t_0) exp\left(-\left({}^{t}/_{\tau}\right)^{\beta}\right) \qquad (2)$$

Also, the regeneration reaction is not expected to follow a stretched exponential function, and comparison of average KWW lifetimes with and without electrolytes can therefore be problematic. Moreover, the average KWW lifetime is calculated using the ill-behaved Γ function. For cases where $\beta < 0.3$, as has been reported for NiO systems,[40] the average lifetimes can be quite large, orders of magnitude larger than the time point at which the original data no longer shows a detectable signal. In such a case the average lifetime

Physical Chemistry Chemical Physics Accepted Manuscript

calculated has no physical relevance. For these reasons we prefer not to use the KWW function here.

The ns-μs kinetic traces for $DPP^{\bullet-}$ and $NDI^{\bullet-}$ decay, with and without $Co^{II/III}$ electrolyte (Figure 10 and S13) were fitted using a biexponential function; the results are tabulated in Table 3. The largest effect of $Co^{II/III}$ is for NiO/DPP-NDI, where $<\tau>$ decreases from 140 μs (see above) to 5.6 μs. Control experiments suggested that addition of $Co^{II/III}$ does not change the recombination kinetics: addition of only Co^{II} has no effect, and addition of only Co^{III} has the same effect as adding both Co^{II} and Co^{III} (Figure S14).[53] Thus, we expect that the faster decay kinetics is entirely due to regeneration of the dye by Co^{III}, which suggests a regeneration efficiency of ≈95% for DPP-NDI. In contrast, the generation of the μs-fraction of DPPBr and DPPCN2 is only ≈65% and ≈35% efficient, respectively. However, the greatest loss for these dyes lies in that the majority of DPP recombines on the time scale of 100 ps.

Table 3. Time constants obtained from a biexponential fit of DPP sensitizers on NiO film, with and without $Co^{III/II}$ electrolyte.

Dye	Elec.[a]	τ_1/μs	A_1 (%)	τ_2/μs	A_2 (%)	$<\tau>^b$/μs
DPPBr	Li (ClO_4)	3.0	40	27	60	11
	$Co^{III/II}$	1.6	63	11	37	5.6
$DPPCN_2$	Li (ClO_4)	1.7	75	28	25	3.4
	$Co^{III/II}$	1.0	71	13	29	2.1
DPP-NDI	Li (ClO_4)	49	37	260	63	140
	$Co^{III/II}$	4.5	92	75	8	5.6

a) Electrolyte: Li(ClO_4) = 0.1 M $LiClO_4$ in propylene carbonate; and $Co^{III/II}$ = 0.1 M $[Co(dtb\text{-}bpy)_3](ClO_4)_{2/3}$ with 0.1 M $LiClO_4$ in propylene carbonate. b) defined in eq. 1.

These dyes have been tested in NiO-based DSSCs with I_3^-/I^- as electrolyte, and the maximum IPCE values were 25% for DPP-NDI, 22% for DPPCN2 and 8% for DPPBr.[30] This trend agrees with that of the charge separation lifetimes observed here, although the small difference between DPP-NDI and DPPCN2 is surprising. However, I_3^-/I^- is a non-trivial electrolyte that may regenerate dyes even on the short ps time scale in both photoanodes[52,54] and photocathode owing to static pre-association of triiodide anion with the dyes.[55] $Co^{II/III}$ on

Physical Chemistry Chemical Physics Accepted Manuscript

the other hand is slower, but gives a much better photovoltage. Indeed the best photovoltaic efficiency was obtained with DPP-NDI and the $Co^{II/III}$ redox couple.[30] The IPCE was still up to 20%, in spite of a more sluggish redox couple. In the present study we see that regeneration of the DPP-NDI is very efficient. Most of the losses can then be expected to occur on the ~10 ps time scale, in the step where recombination of $DPP^{\bullet-}$-NDI competes with charge shift to form the long-lived DPP-$NDI^{\bullet-}$ species. To minimize the primary recombination is therefore the key to obtain high efficiency NiO/dye systems for DSSCs.

Conclusion

Femtosecond and nanosecond transient absorption experiments demonstrate ultrafast hole injection (~200 fs + ps components) of all three DPP dyes to the NiO film. The subsequent charge recombination was found to occur over a remarkably wide range of time scales in each system. For DPPBr and DPPCN2 the main recombination lifetime was ~65 ps and ~150 ps, respectively, yet recombination could still be monitored out to the 10's of μs time scale. This amplifies the results of earlier reports that the kinetic heterogeneity of NiO/dye photocathode systems is much greater than in their more well-known TiO_2 photoanode counterparts, and it extends the time scale of observed recombination to span more than six orders of magnitude. It is clear that studies using only slower methods, such as ns-laser spectroscopy, to study dye-sensitized NiO may miss important parts of the recombination process.

Another important difference from TiO_2/dye systems is the independence of the recombination kinetics on excitation power, in the range examined. These differences underscore the need to develop independent understanding of NiO/dye systems in order to improve photocathode performance in DSSCs.

In DPP-NDI we showed a rapid intramolecular electron transfer (~10 ps) after hole injection: $NiO^{(+)}$/$DPP^{\bullet-}$-NDI => $NiO^{(+)}$/DPP-$NDI^{\bullet-}$. This resulted in a ~10^5-fold increase in average

Physical Chemistry Chemical Physics Accepted Manuscript

charge separation lifetime, up to $<\tau>$ = 140 μs. Addition of a $Co^{II/III}$ electrolyte regenerated the dye in the DPP-$NDI^{\bullet-}$ state with an estimated efficiency of ~95%, which explains previous reports of improved photovoltaic properties for DPP-NDI compared to DPPBr and DPPCN2. The main charge loss appears to be in the competition between the intramolecular electron transfer to the NDI unit and rapid recombination components of the NiO/$DPP^{\bullet-}$-NDI state. Thus, the early recombination phases appears to be the main limiting factor for the performance of NiO/dye DSSCs, as has been suggested in some previous cases.

Acknowledements

The authors are grateful for support from The Swedish Energy Agency, The Knut and Alice Wallenberg Foundation, the ANR program POSITIF (ANR-12-PRGE-0016-01) and Région des Pays de la Loire through the project LUMOMAT and European Commission via the COST CM1202 program (PERSPECT H2O). L. Z. acknowledges Jens Fohlinger, Dr. Abhinandan Makhal and Dr. Jonas Petersson at UU for kind help and funding support from the China Scholarship Council (CSC).

Physical Chemistry Chemical Physics Accepted Manuscript

Endnote and References

[#] Note that the relative magnitude of excited state absorption and emission in a ns-experiment depends on the instrument geometry, and that the resulting magnitude of any spontaneous emission cannot be compared to stimulated emission in a fs-pump-probe experiment.

(1) Morandeira, A.; Boschloo, G.; Hagfeldt, A.; Hammarström, L. Photoinduced ultrafast dynamics of coumarin 343 sensitized p-type-nanostructured. *J. Phys. Chem. B* **2005**, *109*, 19403-19410.

(2) Ji, Z.; Natu, G.; Huang, Z.; Wu, Y. Linker effect in organic donor–acceptor dyes for p-type NiO dye sensitized solar cells. *Energy Environ. Sci.* **2011**, *4*, 2818.

(3) Bian, Z.; Tachikawa, T.; Cui, S.-C.; Fujitsuka, M.; Majima, T. Single-molecule charge transfer dynamics in dye-sensitized p-type NiO solar cells: Influences of insulating Al2O3 layers. *Chem. Sci.* **2012**, *3*, 370.

(4) Odobel, F.; Pellegrin, Y.; Gibson, E. A.; Hagfeldt, A.; Smeigh, A. L.; Hammarström, L. Recent advances and future directions to optimize the performances of p-type dye-sensitized solar cells. *Coord. Chem. Rev.* **2012**, *256*, 2414-2423.

(5) Ji, Z.; He, M.; Huang, Z.; Ozkan, U.; Wu, Y. Photostable p-type dye-sensitized photoelectrochemical cells for water reduction. *J. Am. Chem. Soc.* **2013**, *135*, 11696-11699.

(6) Ji, Z.; Wu, Y. Photoinduced electron transfer dynamics of cyclometalated ruthenium (II)–naphthalenediimide dyad at NiO photocathode. *J. Phys. Chem. C* **2013**, *117*, 18315-18324.

(7) Powar, S.; Daeneke, T.; Ma, M. T.; Fu, D.; Duffy, N. W.; Götz, G.; Weidelener, M.; Mishra, A.; Bäuerle, P.; Spiccia, L.; Bach, U. Highly efficient p-type dye-sensitized solar cells based on tris(1,2-diaminoethane)cobalt(II)/(III) electrolytes. *Angew. Chem., Int. Ed. Engl.* **2013**, *125*, 630-633.

(8) (a) Lefebvre, J. F.; Sun, X. Z.; Calladine, J. A.; George, M. W.; Gibson, E. A. Promoting charge-separation in p-type dye-sensitized solar cells using bodipy. *Chem Commun.* **2014**, *50*, 5258-5260; (b) Wood, C. J.; Cheng, M.; Clark, C. A.; Horvath, R.; Clark, I. P.; Hamilton, M. L.; Towrie, M.; George, M. W.; Sun, L.; Yang, X.; Gibson, E. A., Red-Absorbing Cationic Acceptor Dyes for Photocathodes in Tandem Solar Cells, *J. Phys. Chem. C* **2014**, *118*, 16536−16546.

Physical Chemistry Chemical Physics Accepted Manuscript

(9) Warnan, J.; Pellegrin, Y.; Blart, E.; Zhang, L.; Brown, A.; Hammarström, L.; Jacquemin, D.; Odobel, F. Acetylacetone anchoring group for NiO-based dye-sensitized solar cell. *Dyes. Pigments* **2014**, *105*, 174-179.

(10) Daeneke, T.; Yu, Z.; Lee, G. P.; Fu, D.; Duffy, N. W.; Makuta, S.; Tachibana, Y.; Spiccia, L.; Mishra, A.; Bäuerle, P.; Bach, U. Dominating energy losses in NiO p-type dye-sensitized solar cells. *Adv. En. Mater.* **2015**, *5*, 1401387

(11) Perera, I. R.; Daeneke, T.; Makuta, S.; Yu, Z.; Tachibana, Y.; Mishra, A.; Bauerle, P.; Ohlin, C. A.; Bach, U.; Spiccia, L. Application of the tris(acetylacetonato)iron(III)/(II) redox couple in p-type dye-sensitized solar cells. *Angew. Chem., Int. Ed. Engl.* **2015**, *54*, 3758-3762.

(12) Sheibani, E.; Zhang, L.; Liu, P.; Xu, B.; Mijangos, E.; Boschloo, G.; Hagfeldt, A.; Hammarström, L.; Kloo, L.; Tian, H. A study of oligothiophene–acceptor dyes in p-type dye-sensitized solar cells. *RSC Adv.* **2016**, *6*, 18165-18177.

(13) Odobel, F.; Pellegrin, Y. Recent advances in the sensitization of wide-band-gap nanostructured p-type semiconductors. Photovoltaic and photocatalytic applications. *J. Phys. Chem. Lett.* **2013**, *4*, 2551-2564.

(14) Odobel, F.; Le Pleux, L.; Pellegrin, Y.; Blart, E. New photovoltaic devices based on the sensitization of p-type semiconductors: Challenges and opportunities. *Acc. Chem. Res.* **2010**, *43*, 1063-1071.

(15) Gardner, J. M.; Beyler, M.; Karnahl, M.; Tschierlei, S.; Ott, S.; Hammarstrom, L. Light-driven electron transfer between a photosensitizer and a proton-reducing catalyst co-adsorbed to NiO. *J. Am. Chem. Soc.* **2012**, *134*, 19322-19325.

(16) Kamat, P. V. Meeting the clean energy demand: Nanostructure architectures for solar energy conversion. *J. Phys. Chem. C* **2007**, *111*, 2834-2860.

(17) Click, K. A.; Beauchamp, D. R.; Huang, Z.; Chen, W.; Wu, Y. Membrane-inspired acidically stable dye-sensitized photocathode for solar fuel production. *J. Am. Chem. Soc.* **2016**, *138*, 1174-1179.

(18) Ji, Z.; He, M.; Huang, Z.; Ozkan, U.; Wu, Y. Photostable p-type dye-sensitized photoelectrochemical cells for water reduction. *J. Am. Chem. Soc.* **2013**, *135*, 11696-11699.

Physical Chemistry Chemical Physics Accepted Manuscript

(19) He, J.; Lindström, H.; Hagfeldt, A.; Lindquist, S.-E. Dye-sensitized nanostructured tandem cell-first demonstrated cell with a dye-sensitized photocathode. *Sol. Energ. Mater. Sol. Cells.* **2000**, *62*, 265-273.

(20) Nakasa, A.; Usami, H.; Sumikura, S.; Hasegawa, S.; Koyama, T.; Suzuki, E. A high voltage dye-sensitized solar cell using a nanoporous nio photocathode. *Chem. Lett.* **2005**, *34*, 500-501.

(21) Qin, P.; Zhu, H.; Edvinsson, T.; Boschloo, G.; Hagfeldt, A.; Sun, L. Design of an organic chromophore for p-type dye-sensitized solar cells. *J. Am. Chem. Soc.* **2008**, *130*, 8570-8571.

(22) Gibson, E. A.; Smeigh, A. L.; Le Pleux, L.; Fortage, J.; Boschloo, G.; Blart, E.; Pellegrin, Y.; Odobel, F.; Hagfeldt, A.; Hammarstrom, L. A p-type nio-based dye-sensitized solar cell with an open-circuit voltage of 0.35 V. *Angew. Chem., Int. Ed. Engl.* **2009**, *48*, 4402-4405.

(23) Nattestad, A.; Mozer, A. J.; Fischer, M. K. R.; Cheng, Y. B.; Mishra, A.; Bäuerle, P.; Bach, U. Highly efficient photocathodes for dye-sensitized tandem solar cells. *Nature Mater.* **2009**, *9*, 31-35.

(24) Qin, P.; Linder, M.; Brinck, T.; Boschloo, G.; Hagfeldt, A.; Sun, L. High incident photon-to-current conversion efficiency of p-type dye-sensitized solar cells based on NiO and organic chromophores. *Adv. Mater.* **2009**, *21*, 2993-2996.

(25) Gibson, E. A.; Smeigh, A. L.; Le Pleux, L.; Hammarström, L.; Odobel, F.; Boschloo, G.; Hagfeldt, A. Cobalt polypyridyl-based electrolytes for p-type dye-sensitized solar cells. *J. Phys. Chem. C,* **2011**, *115*, 9772-9779.

(26) Powar, S.; Daeneke, T.; Ma, M. T.; Fu, D.; Duffy, N. W.; Götz, G.; Weidelener, M.; Mishra, A.; Bäuerle, P.; Spiccia, L.; Bach, U. Highly efficient p-type dye-sensitized solar cells based on tris(1,2-diaminoethane)cobalt(ii)/(iii) electrolytes. *Angew. Chem., Int. Ed.* **2013**, *52*, 602-605.

(27) Perera, I. R.; Daeneke, T.; Makuta, S.; Yu, Z.; Tachibana, Y.; Mishra, A.; Bäuerle, P.; Ohlin, C. A.; Bach, U.; Spiccia, L. Application of the tris(acetylacetonato)iron(III)/(II) redox couple in p-type dye-sensitized solar cells. *Angew. Chem., Int. Ed. Engl.* **2015**, *54*, 3758-3762.

(28) Morandeira, A.; Fortage, J.; Edvinsson, T.; Le Pleux, L.; Blart, E.; Boschloo, G.; Hagfeldt, A.; Hammarström, L.; Odobel, F. Improved photon-to-current conversion efficiency with a nanoporous p-type NiO electrode by the use of a sensitizer-acceptor dyad. *J. Phys. Chem. C* **2008**, *112*, 1721-1728.

Physical Chemistry Chemical Physics Accepted Manuscript

(29) Nattestad, A.; Mozer, A. J.; Fischer, M. K. R.; Cheng, Y. B.; Mishra, A.; Baeuerle, P.; Bach, U. Highly efficient photocathodes for dye-sensitized tandem solar cells. *Nature Mater.* **2010**, *9*, 31-35.

(30) Favereau, L.; Warnan, J.; Pellegrin, Y.; Blart, E.; Boujtita, M.; Jacquemin, D.; Odobel, F. Diketopyrrolopyrrole derivatives for efficient NiO-based dye-sensitized solar cells. *Chem. Commun.* **2013**, *49*, 8018-8020.

(31) Sumikura, S.; Mori, S.; Shimizu, S.; Usami, H.; Suzuki, E. Syntheses of NiO nanoporous films using nonionic triblock co-polymer templates and their application to photo-cathodes of p-type dye-sensitized solar cells. *Journal of Photochemistry and Photobiology A: Chemistry* **2008**, *199*, 1-7.

(32) El-Zohry, A.; Orthaber, A.; Zietz, B. Isomerization and aggregation of the solar cell dye D149. *J. Phys. Chem. C,* **2012**, *116*, 26144-26153.

(33) Petersson, J.; Eklund, M.; Davidsson, J.; Hammarstrom, L. Ultrafast electron transfer dynamics of a Zn(II)porphyrin-viologen complex revisited: S2 vs S1 reactions and survival of excess excitation energy. *J. Phys. Chem. B* **2010**, *114*, 14329-14338.

(34) Pandit, B.; Luitel, T.; Cummins, D. R.; Thapa, A. K.; Druffel, T.; Zamborini, F.; Liu, J. Spectroscopic investigation of photoinduced charge-transfer processes in FTO/TiO2/N719 photoanodes with and without covalent attachment through silane-based linkers. *J. Phys. Chem. A* **2013**, *117*, 13513-13523.

(35) Piatkowski, P.; Martin, C.; di Nunzio, M. R.; Cohen, B.; Pandey, S.; Hayse, S.; Douhal, A. Complete photodynamics of the efficient YD2-o-C8-based solar cell. *J. Phys. Chem. C* **2014**, *118*, 29674-29687.

(36) Warnan, J.; Gardner, J.; Le Pleux, L.; Petersson, J.; Pellegrin, Y.; Blart, E.; Hammarström, L.; Odobel, F. Multichromophoric sensitizers based on squaraine for NiO based dye-sensitized solar cells. *J. Phys. Chem. C* **2014**, *118*, 103-113.

(37) di Nunzio, M. R.; Cohen, B.; Pandey, S.; Hayse, S.; Piani, G.; Douhal, A. Spectroscopy and dynamics of YD2-o-C8 in solution and interacting with alumina nanoparticles electrode. *J. Phys. Chem. C* **2014**, *118*, 11365-11376.

Physical Chemistry Chemical Physics Accepted Manuscript

(38) Johansson, O.; Borgström, M.; Lomoth, R.; Palmblad, M.; Bergquist, J.; Hammarström, L.; Sun, L.; Åkermark, B. Electron donor-acceptor dyads based on ruthenium(II) bipyridine and terpyridine complexes bound to naphthalenediimide. *Inorg. Chem.* **2003**, *42*, 2908-2918.

(39) El-Zohry, A. M.; Roca-Sanjuán, D.; Zietz, B. Ultrafast twisting of the indoline donor unit utilized in solar cell dyes: Experimental and theoretical studies. *J. Phys. Chem. C* **2015**, *119*, 2249-2259.

(40) D'Amario, L.; Antila, L. J.; Pettersson Rimgard, B.; Boschloo, G.; Hammarström, L. Kinetic evidence of two pathways for charge recombination in nio-based dye-sensitized solar cells. *J. Phys. Chem. Lett.* **2015**, *6*, 779-783.

(41) Nelson, J.; Haque, S. A.; Klug, D. R.; Durrant, J. R. Trap-limited recombination in dye-sensitized nanocrystalline metal oxide electrodes. *Phys. Rev. B* **2001**, *63*.

(42) Willis, R. L.; Olson, C.; O'Regan, B.; Lutz, T.; Nelson, J.; Durrant, J. R. Electron dynamics in nanocrystalline ZnO and TiO2 films probed by potential step chronoamperometry and transient absorption spectroscopy. *J. Phys. Chem. B* **2002**, *106*, 7605-7613.

(43) Green, A. N.; Palomares, E.; Haque, S. A.; Kroon, J. M.; Durrant, J. R. Charge transport versus recombination in dye-sensitized solar cells employing nanocrystalline TiO2 and SnO2 films. *J. Phys. Chem. B* **2005**, *109*, 12525-12533.

(44) Makuta, S.; Liu, M.; Endo, M.; Nishimura, H.; Wakamiya, A.; Tachibana, Y. Photo-excitation intensity dependent electron and hole injections from lead iodide perovskite to nanocrystalline tio and spiro-ometad. *Chem Commun.* **2016**, *52*, 673-676.

(45) Haque, S. A.; Tachibana, Y.; Willis, R. L.; Moser, J. E.; Grätzel, M.; Klug, D. R.; Durrant, J. R. Parameters influencing charge recombination kinetics in dye-sensitized nanocrystalline titanium dioxide films. *J. Phys. Chem. B* **2000**, *104*, 538-547.

(46) Morandeira, A.; Fortage, J.; Edvinsson, T.; Le Pleux, L.; Blart, E.; Boschloo, G.; Hagfeldt, A.; Hammarström, L.; Odobel, F. Improved photon-to-current conversion efficiency with a nanoporous p-type nio electrode by the use of a sensitizer-acceptor dyad. *J. Phys. Chem. C* **2008**, *112*, 1721-1728.

(47) Marcus, R. A.; Sutin, N. Electron transfers in chemistry and biology. *Biochim. Biophys. Acta,* **1985**, *811*, 265-322.

Physical Chemistry Chemical Physics Accepted Manuscript

(48) Closs, G. L.; Miller, J. R. Intramolecular long-distance electron transfer in organic molecules. *Science* **1988**, *240*, 440-447.

(49) Ellis, H.; Schmidt, I.; Hagfeldt, A.; Wittstock, G.; Boschloo, G. Influence of dye architecture of triphenylamine based organic dyes on the kinetics in dye-sensitized solar cells. *J. Phys. Chem. C* **2015**, *119*, 21775-21783.

(50) Berberan-Santos, M. N.; Bodunov, E. N.; Valeur, B. Mathematical functions for the analysis of luminescence decays with underlying distributions 1. Kohlrausch decay function (stretched exponential). *Chem. Phys.* **2005**, *315*, 171-182.

(51) Nelson, J.; Chandler, R. E. Random walk models of charge transfer and transport in dye sensitized systems. *Coordin. Chem. Rev.* **2004**, *248*, 1181-1194.

(52) Ardo, S.; Meyer, G. J. Photodriven heterogeneous charge transfer with transition-metal compounds anchored to TiO2 semiconductor surfaces. *Chem. Soc. Rev.* **2009**, *38*, 115-164.

(53) Farré, Y.; Zhang, L.; Pellegrin, Y.; Planchat, A.; Blart, E.; Boujtita, M.; Hammarström, L.; Jacquemin, D.; Odobel, F. Second generation of diketopyrrolopyrrole dyes for NiO based dye-sensitized solar cells. *J. Phys. Chem. C* **2016**, *accepted.*

(54) Antila, L. J.; Myllyperkio, P.; Mustalahti, S.; Lehtivuori, H.; Korppi-Tommola, J. Injection and ultrafast regeneration in dye-sensitized solar cells. *J. Phys. Chem. C* **2014**, *118*, 7772-7780.

(55) Morandeira, A.; Boschloo, G.; Hagfeldt, A.; Hammarström, L. Coumarin 343−NiO films as nanostructured photocathodes in dye-sensitized solar cells: Ultrafast electron transfer, effect of the I3−/I−redox couple and mechanism of photocurrent generation. *J. Phys. Chem. C* **2008**, *112*, 9530-9537.

Physical Chemistry Chemical Physics Accepted Manuscript

Graphical abstract for Entry for

Ultra-fast and Slow Charge Recombination Dynamics of Diketopyrrolopyrrole-NiO Dye Sensitized Solar Cells

Lei Zhang[a], Ludovic Favereau[b], Yoann Farré,[b] Edgar Mijangos[a], Yann Pellegrin,[b] Errol Blart,[b] Fabrice Odobel[b]* and Leif Hammarström[a]*

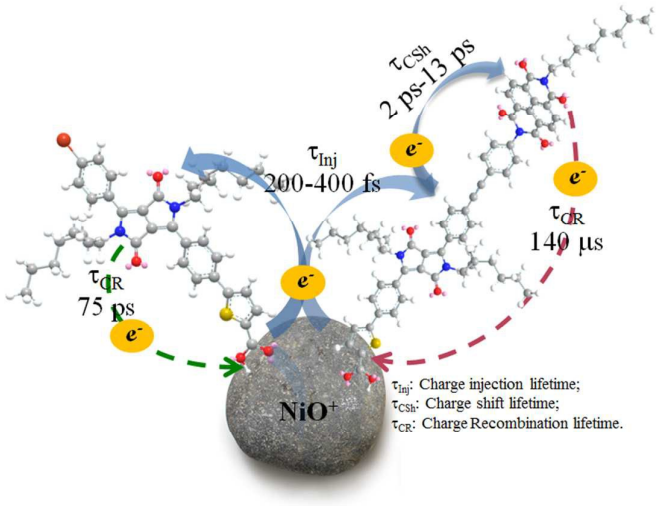

Physical Chemistry Chemical Physics Accepted Manuscript